frontiers | Frontiers in Earth Science

TYPE Original Research
PUBLISHED 24 August 2023
DOI 10.3389/feart.2023.1242567

OPEN ACCESS

EDITED BY
Dawei Fan,
Chinese Academy of Sciences (CAS), China

REVIEWED BY
Jinze Xu,
University of Calgary, Canada
Hu Li,
Southwest Petroleum University, China

*CORRESPONDENCE
Liangbin Dou,
doulb@xsyu.edu.cn

RECEIVED 23 June 2023
ACCEPTED 07 August 2023
PUBLISHED 24 August 2023

CITATION
Dou L, Chen J, Zuo X, Liu Y, Sun L, Fang Y, Cheng X and Wang T (2023), Comparison of mechanical characteristics of different types of shales in the Ordos Basin. *Front. Earth Sci.* 11:1242567. doi: 10.3389/feart.2023.1242567

Comparison of mechanical characteristics of different types of shales in the Ordos Basin

Liangbin Dou[1,2,3]*, Jingyang Chen[1,3], Xiongdi Zuo[1,3], Yonghui Liu[4], Lin Sun[5], Yong Fang[1,3], Xuebin Cheng[1,3] and Ting Wang[1,3]

[1]College of Petroleum Engineering, Xi'an Shiyou University, Xi'an, Shaanxi, China, [2]Key Laboratory of Unconventional Oil and Gas Development [China University of Petroleum (East China)], Ministry of Education, Qingdao, China, [3]Engineering Research Center for Development and Management of Western Low-Permeability and Ultra-Low Permeability Oilfield, Ministry of Education, Xi 'an Shiyou University, Xi'an, Shaanxi, China, [4]Longdong Oil and Gas Development Branch of Changqing Oilfield, Qingyang, Gansu, China, [5]Bohai Drilling Third Drilling Company of China Petroleum Group, Tianjin, China

Shale gas is a very important unconventional energy. The mechanical properties of the three types of shale (laminated shale, sandwich shale and foliated shale) are different, and the difference in fracturing effectiveness is very significant. In this paper, the mineral composition, mechanical properties and conductivity of these three different types of shale were studied and compared by X-ray diffraction, triaxial mechanical experiments, and fracture conduction experiments. The study found that the foliated shale has the lowest content of rigid minerals (47.5%), lower elastic modulus and tensile strength (26.98 Gpa and 168.29 MPa, respectively), higher Poisson's ratio (0.25), the smallest brittleness index (0.48), and larger fracture toughness (0.42). The laminated shale has a higher content of rigid minerals (68.50%), the lowest elastic modulus and tensile strength (25.77 Gpa and 122.46 MPa, respectively), the highest Poisson's ratio (0.26), the highest brittleness index (0.56), and the lowest fracture toughness (0.18). The sandwich shale has the highest rigid mineral content (78.16%), the highest elastic modulus and tensile strength (35.31 Gpa and 197.37 MPa, respectively), the lowest Poisson's ratio (0.24), a larger brittleness index (0.52), and larger fracture toughness (0.415). Furthermore, with the increase in the coring angle, the elastic modulus of all three shales increases. In addition, with the increase in closing pressure and the decrease in the sand laying concentration, the proppant embedding depth gradually increases and the conductivity decreases. This means that from the perspective of forming complex fracture networks, the fracturing effect of the foliated shale is unsatisfactory, while the fracturing effect of the laminated and sandwich shales is better. Moreover, it is recommended to prefer directional injection along vertical laminae or at high angles, which is conducive to the formation of complex fracture networks. For laminated shale with low strength, the sand laying concentration should be increased to ensure the conductivity of the fractured fracture. This study provides some technical guidance for the identification of different types of shale fracturing desserts and fracturing processes.

KEYWORDS

laminated shale, sandwich shale, foliated shale, fracturing, mechanical properties, conductivity

1 Introduction

Generally, the porosity and permeability of shale reservoirs are extremely low, so it is difficult to develop shale resources efficiently by relying on the natural porosity and pressure of strata. In most cases, it is necessary to transform shale reservoirs. Rock mechanics parameters are important parameters to evaluate geological conditions, and parameters such as elastic modulus, rock strength, and the brittleness index of shale have a certain indication of fracture extension (Dou et al., 2021a; Dou et al., 2022a; Dou et al., 2022b). Depending on the composition and structure of the shale, shales are commonly classified into three types: laminated, sandwich, and foliated shales. Laminated shale is mainly characterized by interbedding of thin mudstone and fine sandstone. Foliated shale is mainly thick-layered shale with a small amount of siltstone, and the foliated joints in the middle layer of shale are well-developed. Sandwich shale is characterized by interbedding of thick mudstone and fine sandstone.

Regarding laminated shale, in 2021, Jia Jiasheng, Tan P, and others studied the brittleness of laminated shale, which showed that with the increase in the confining pressure, the anisotropy of shale decreased, with the obvious decrease in the brittleness. When the bedding dip angle increased, the brittleness of shale decreased first and then increased (Tan et al., 2017; Jia et al., 2021). In 2021, Zhao Xiaoxiao and others studied and analyzed marine shale, and determined that there were five types of laminae in the study area. Among them, the organic-rich siliceous lamination had high uniaxial compressive strength and Young's modulus, which had good physical properties and development potential, and it was concluded that the elastic modulus and strength of rocks were greater when they were parallel to the bedding direction (Liang et al., 2021; Zhao et al., 2021). In 2022, Xiong Min, Lee J S, and others studied the characteristics of marine shale laminae, showing that marine shale laminae were formed by different hydrodynamic conditions, and the diversity of laminae affected the reservoir space and pore structure, resulting in strong heterogeneity (Lee et al., 2014; Zhu et al., 2019; Xiong et al., 2022). In 2023, Song Siyu's study on shale texture types in the Konger second member of the Cangdong Depression and its influence on reservoir performance showed that the shale texture mainly includes three structural types: the felsic–carbonate–clay texture, felsic–carbonate–clay mineral texture, and clay–carbonate–analcime texture. Different structural types have different influences on shale reservoir performance, and the felsic–carbonate–clay mineral type is the best. The clay–carbonate–analcime type is the weakest (Gallant et al., 2007; Xin et al., 2022; Song et al., 2023).

For sandwich shale, in the study on the definition standard and main control factors of sandwich shale oil in the first member of the Shahejie Formation in the Bonan Depression in Zhu Deshun in 2015, sandwich shale oil was mainly in the free state, which is controlled by sandwich thickness, reservoir physical properties, and formation pressure. The greater the thickness of a single sandwich shale, the higher the shale oil production (Zhu et al., 2015; Shen et al., 2022). In 2019, Liu Yali studied the characteristics and functions of sandwich shale in continental organic-rich mud shale, and concluded that sandwich shale in this area mainly comprises sandstone, limestone, and dolomite, and at the same time, the sandwich shales contain a large number of brittle minerals, which is beneficial for fracturing and reconstruction (Wang et al., 2018c; Fu et al., 2019; Liu and Liu, 2019). In 2022, Pang Zhenglian studied the sandwich shale in the seventh member of the Yanchang Formation in the Ordos Basin, which showed that the sandwich shale had strong heterogeneity (Pang et al., 2023). In 2022, Tang Xinping and others studied the limestone sandwich shale in the second member of the Bu 'er Formation in the Sanshui Basin and concluded that the sandwich shale in this area has the main reservoir space of matrix pore-fractures, good reservoir properties, brittleness and oil-bearing properties, and good reservoir-forming conditions (Tang et al., 2022). In 2022, Zhao Xiaoxiao and others studied the lacustrine shale of the Shahejie Formation in the Zhanhua Depression and analyzed that this area mainly contains sandwich shale, in which brittle minerals are high in content and fractures are more likely to form. The reservoir space includes intergranular pores, intragranular dissolution pores, intergranular pores, and microfractures (Zhao et al., 2022; Zhang et al., 2023). In 2023, Du Xunshe, Wang J, and others studied the sandwich shale oil of the Chang seventh member in the Longdong area. The maturity of the shale in the study area is low, the reservoir space consists of dissolution pores and intergranular pores, and the lithology is mainly fine-grained lithic feldspathic sandstone and feldspathic lithic sandstone (Wang J. et al., 2018; Sun et al., 2021; Du, 2023).

Regarding foliated shale, Wakabayashi J et al. and Liu Shuanglian et al. studied the influence of foliation on the logging response and rock mechanics parameters in 2019, and found that in logging, acoustic wave velocity and Young's modulus decreased with the increase in the foliation density, Poisson's ratio decreased with the increase in the foliation density when the foliation angle was less than 45, and Young's modulus increased with the increase in the foliation angle when it exceeded 45 (Wakabayashi and Dilek, 2011; Cho et al., 2012; Liu, 2019). In 2021, Liu Bo, Camargo JAJ, and others conducted relevant research on foliated shale, which proved that foliated shale usually contains higher organic matter abundance and a high pressure coefficient, which is more conducive to oil and gas accumulation. At the same time, its brittleness index is usually lower than that of laminated shale (Liu et al., 2021; Camargo et al., 2022). In 2021, Jingru Yang and others studied the classification characteristics of shale foliation, primarily analyzed the fractal factors of shale reservoirs, described the heterogeneity of shale foliation, and studied its influence on fracture propagation (Valdiviezo-Mijangos and Nicolás-Lopez, 2014; Ruggieri et al., 2021; Xu et al., 2021; Yang et al., 2021).

In a word, at present, most of the research is aimed at a single type of shale, and there is still a lack of comparative research on rock characteristics between different shales in the same area (Horsrud, 2001; Zhang et al., 2006; Simpson et al., 2014). In this paper, by comparing the mineral composition, elastic modulus, and Poisson's ratio of the three kinds of shales in the study area, the strength characteristics of different types of shales and different coring angles are determined, their brittleness distribution is analyzed, and the specific fracturing technology for different types of shales is obtained, thus effectively improving reservoir porosity, permeability, and ultimate recovery (da Silva et al., 2008; Dou et al., 2021b; Dou et al., 2021c).

FIGURE 1
Different types of shale in the study area. **(A)** Sandwich Shale, **(B)** Laminated Shale, **(C)** Foliated Shale.

TABLE 1 Comparison of mineral components in different areas.

Area	Rock type	Mineral content/%						Remarks
		Rigid component					Clay %	
		Quartz %	Feldspar %	Carbonate %	Pyrite %	Total %		
Li 57 Block, Chang 7_3, Longdong	Foliated shale	33.60	13.00	0.90	/	47.50	52.50	
Mu 14 Block, Chang 7_3, Longdong	Laminated shale	46.30	11.90	5.20	5.10	68.50	31.50	
Gao 62 Block, Chang 7_3, Northern Shaanxi	Sandwich shale	29.40	41.46	7.30	/	78.16	21.84	
Longmaxi Formation, Sichuan	Siliceous shale	43.86	25.38	3.38	0.23	72.85	27.15	Wang et al. (2018b)
Niutitang Formation	Silty shale	42.96	15.94	8.06	1.42	68.38	31.62	Tian et al. (2018)
Barnett	Siliceous shale	45.00	7.00	8.00	5.00	65.00	32.00	Yang et al. (2016)
Eagle Ford	Calcareous shale	4.70	8.90	53.50	2.40	69.50	30.40	

2 Distribution of shale in the Ordos Basin

According to the experience of shale oil and gas exploration and development in North America, shale rocks rich in brittle minerals such as quartz and carbonate have better fracturability and are conducive to the formation of natural fractures and induced fractures under the action of external forces which are favorable for shale oil development. According to the differences in shale components and structures, the shales in the study area are divided into three types: foliated, laminated, and sandwich shales. As shown in Figure 1A, the Chang-7 shale in northern Shaanxi is dominated by

10.3389/feart.2023.1242567

TABLE 2 Statistics of the mechanical properties of different types of rocks.

Test type	Rock type	Maximum	Minimum	Average value
Elastic modulus/Gpa	Sandwich shale	42.22	24.45	35.31
	Foliated shale	36.90	17.50	26.98
	Laminated shale	37.52	9.01	25.77
	Sandstone	45.04	22.69	33.74
Poisson's ratio	Sandwich shale	0.29	0.20	0.24
	Foliated shale	0.28	0.19	0.25
	Laminated shale	0.37	0.20	0.26
	Sandstone	0.31	0.23	0.26
Compressive strength/MPa	Sandwich shale	248.30	160.44	197.37
	Foliated shale	231.48	126.93	168.29
	Laminated shale	194.99	70.92	122.46
	Sandstone	310.25	144.40	193.94

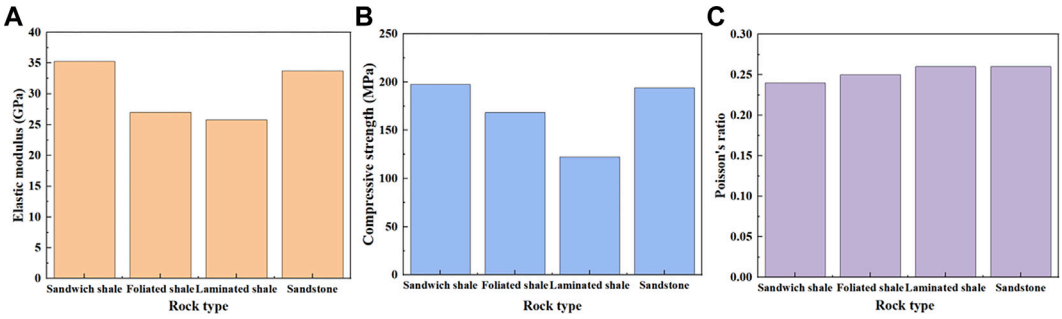

FIGURE 2
Comparison of mechanical properties of different types of rocks. **(A)** Elastic modulus, **(B)** Compressive strength, **(C)** Poisson's ratio.

sandwich shale. Sandwich shale is mainly characterized by the interbedding development of thick mudstone and fine sandstone. According to the statistics of sandstone and mudstone thickness in the core box of the coring interval, it is found that the mudstone section is thin, with the mudstone thickness ranging from 0.20 to 0.60 m, and the mudstone section accounts for 11.11%–33.35% of the observed core box length. There are two different types of shales in Longdong, namely, laminated and foliated shales, as shown in Figure 1B, C. Laminated shale is mainly composed of thin mudstone and fine-grained sandstone, and the thickness of mudstone and fine-grained sandstone is mostly between 0.60 and 1.30 cm. The thickness of mudstone or fine-grained sandstone in some intervals is relatively large, and the maximum thickness of fine-grained sandstone can reach 7.35 cm, while that of mudstone can reach 2.38 cm. The foliated shale is mainly developed in thick-bedded shale, and siltstone and other lithology are rare in the core box. In shale, bedding fissure is well developed, with the highest density of foliated joints being 81/m, the width of foliated joints ranging from 0.1 to 0.5 mm, and the length of foliated joints ranging from 1.0 to 9.6 cm.

3 Experiment on mineral composition

The mineral components of shale in the Ordos Basin were measured using an X-ray diffractometer (XRD-6000) with the standard SY/T 5163–2018 (Teng et al., 2022). The experimental results are shown in Table 1 and compared with shale mineral components from other areas.

As shown in Table 1, the reservoir in the study area is mainly composed of quartz, feldspar (potassium feldspar and plagioclase), carbonate (calcite, dolomite, and siderite), pyrite, and clay (illite, chlorite, and illite-montmorillonite mixed layer). Among them, the content of clay minerals in foliated shale is the highest (52.5%), the content of quartz in laminated shale is the highest (46.3%), and the content of feldspar in sandwich shale is the highest (41.46%).

The content of rigid minerals such as quartz, feldspar, carbonate, and pyrite can reflect the brittleness of the reservoir. The higher the content of rigid minerals is, the higher the brittleness of the reservoir. Among the three types of shale, the highest content of rigid minerals in sandwich shale is 78.16%, which is closer to the content of rigid minerals in the siliceous shale of the Longmaxi Formation in Sichuan (Wang K. et al., 2018), which is favorable for

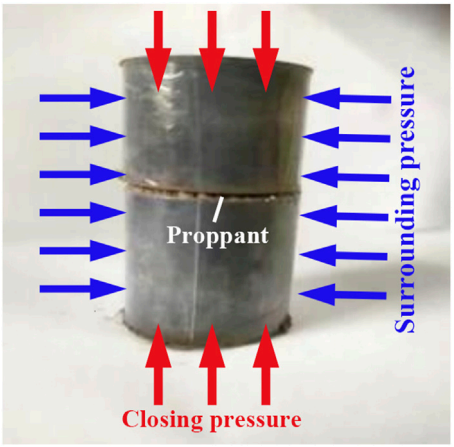

FIGURE 3
Experimental samples of the proppant embedded.

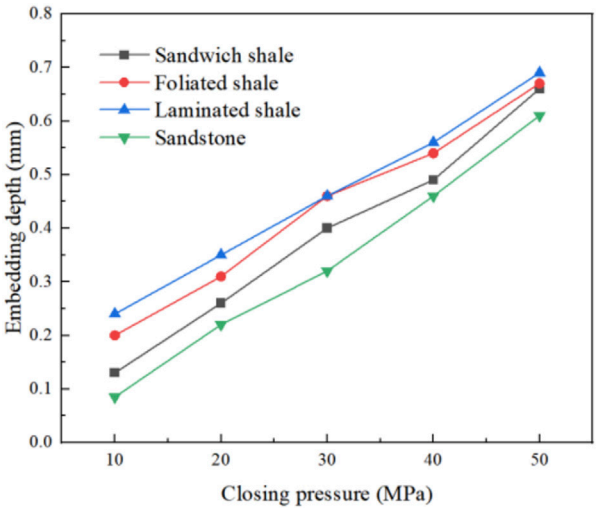

FIGURE 4
Influence of closing pressure on the embedding depth.

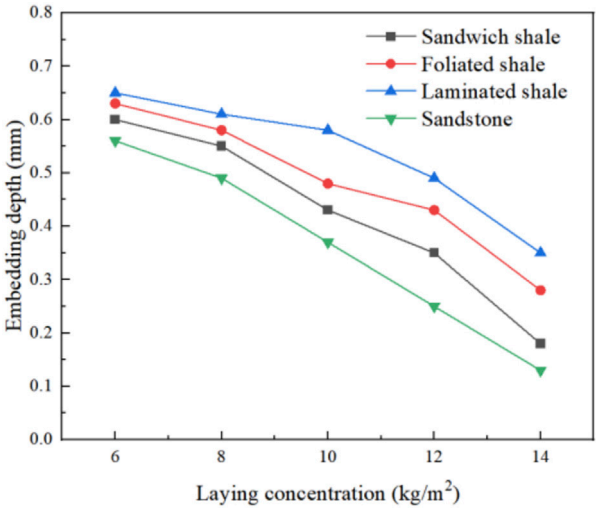

FIGURE 5
Influence of the laying concentration on the embedding depth.

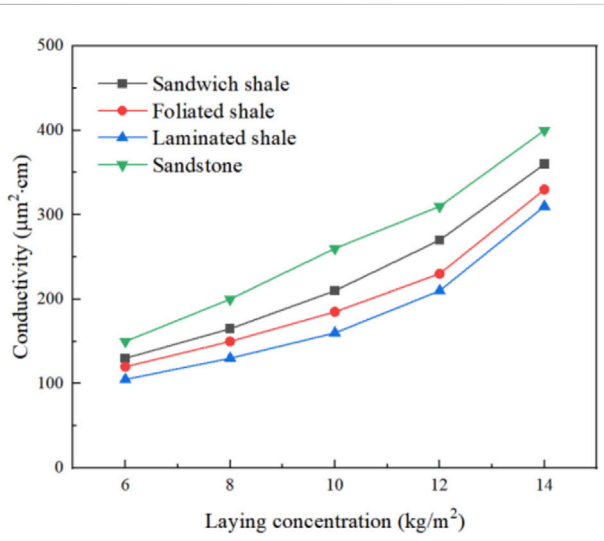

FIGURE 6
Conductivity under different laying concentrations.

shale oil and gas storage and has better fracturability. The content of rigid minerals in the laminated shale is 68.5%, which is similar to that of the silty shale of the Niutitang Formation, the siliceous shale of the Barnett, and the calcareous shale of the Eagle Ford (Yang et al., 2016; Tian et al., 2018). The content of rigid minerals in foliated shale is the lowest, which is only 47.5%. Therefore, the foliated shale is the least brittle, and the sandwich and laminated shales are more brittle and more likely to form complex fracture networks during the fracturing of shale reservoirs.

4 Experiment on mechanical properties

The mechanical properties of 30 shales in the study area are evaluated using the TAW-1000 servo-controlled triaxial rock mechanics experimental system. The experimental core size is Φ25 × 50 mm, and the loading rate is 0.02 mm/min. The elastic modulus, Poisson's ratio, and compressive strength of different types of rocks are tested according to GB/T 235619-2009 "Determination Methods of Physical and Mechanical Properties of Coal and Rock." The experimental steps are as follows: 1) First, the temperature and pore pressure are applied. Then, the liquid confining pressure is applied to the cylindrical core transversely, and then, the axial load is gradually increased to measure the axial stress when the rock is destroyed, and the stress–strain relationship curve is drawn; 2) based on the experimental results and acoustic characteristics of static and dynamic rock mechanics under the same conditions, the dynamic and static transformation relationship under the actual formation confining pressure is constructed. 3) The tensile strength of rock is

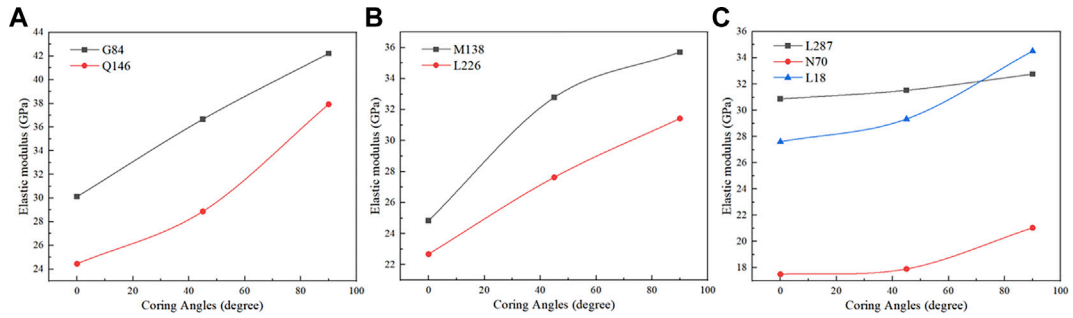

FIGURE 7
Influence of coring angle on elastic modulus of different shale types. **(A)** Sandwich Shale, **(B)** Laminated Shale, **(C)** Foliated Shale.

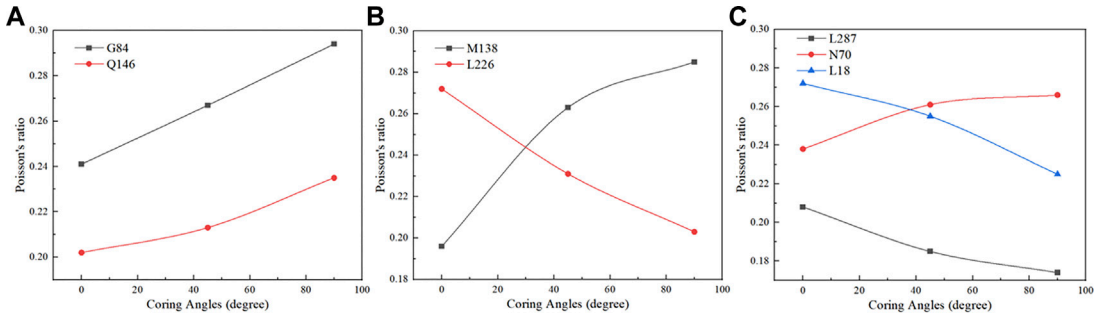

FIGURE 8
Influence of coring angle on Poisson's ratio of different shale types. **(A)** Sandwich Shale, **(B)** Laminated Shale, **(C)** Foliated Shale.

TABLE 3 Comparison of the brittleness indices of different types of shales.

Shale type	Block	Brittleness index		
		Maximum	Minimum	Average value
Sandwich shale	Q146	0.62	0.09	0.40
	G68	0.88	0.05	0.56
	G84	0.90	0.12	0.59
	Average	-	-	0.52
Foliated shale	M53	0.68	0.05	0.40
	L287	0.88	0.12	0.55
	Average	-	-	0.48
Laminated shale	M138	0.88	0.05	0.52
	L226	0.85	0.13	0.60
	Average	-	-	0.56

indirectly measured through the tensile test of rock. Table 2 shows the statistics of the results. For sandwich shale, the elastic modulus is between 24.45 and 42.22 Gpa, with an average of 35.31 Gpa; the Poisson's ratio ranges from 0.20 to 0.29, with an average of 0.24; and the compressive strength ranges from 160.44 to 248.30 MPa, with an average of 197.37 MPa. For foliated shale, the elastic modulus is between 17.50 and 36.90 Gpa, with an average of 26.98 Gpa; the Poisson's ratio ranges from 0.19 to 0.28, with an average of 0.25; and the compressive strength ranges from 126.93 to 231.48 MPa, with an average of 168.29 MPa. For laminated shale, the elastic modulus is between 9.01 and 37.52 Gpa, with an average of 25.77 Gpa; the Poisson's ratio ranges from 0.20 to 0.37, with an average of 0.26; and the compressive strength ranges from 70.92 to 194.99 MPa, with an average of 122.46 MPa. The comparison of the mechanical properties of different types of rocks is shown in Figure 2.

As shown in Figures 2A, B, the elastic modulus and compressive strength of the sandwich shale are the highest and higher than those of the sandstone, which makes it more difficult for fractures to expand during the fracturing process and forms a relatively single fracture network. The elastic modulus and compressive strength of the foliated shale are the second highest and lower than those of sandstone. The elastic modulus and compressive strength of the laminated shales are the lowest. This makes the fracturing process easier to initiate fractures, and it is relatively easy for fracture expansion to communicate with natural fractures (shale develops weak planes such as laminations and fractures) under the same net pressure conditions, making it easier to form a complex fracture network. As shown in Figure 2C, the Poisson's ratio of laminated shale is the highest and is equal to that of sandstone. The Poisson's ratio of foliated shale is the second highest, and the Poisson's ratio of sandwich shale is the lowest. According to the

TABLE 4 Comparison of the fracture toughness of different types of shales.

Shale type	Block	Fracture toughness		
		K_{IC}/MPa·m$^{0.5}$	K_{IIC}/MPa·m$^{0.5}$	K_n
Sandwich shale	Q146	6.81	2.05	0.15
	G68	6.81	2.05	0.15
	G84	8.34	2.47	0.25
	Average	7.32	2.19	0.18
Foliated shale	M53	11.18	3.40	0.46
	L287	9.70	3.09	0.38
	Average	10.44	3.25	0.42
Laminated shale	M138	10.03	3.41	0.44
	L226	9.55	3.18	0.39
	Average	9.79	3.30	0.415

mechanical properties of rocks, the laminae and foliated shale should be chosen for fracturing development.

5 Experiment on fracture conductivity

5.1 Proppant embedment

During the process of shale fracturing, the fracturing fluid enters the shale reservoir and interacts with various minerals in the shale, thereby changing the original pore structure of the shale and reducing its mechanical properties, increasing the degree to which the fractured fracture is embedded by the proppant, and thus affecting the conductivity of the fractured fractures. Therefore, it is required to soak the experimental cores in the fracturing fluid for 72 h before the proppant embedment experiment.

The uniaxial/triaxial compression test module of the GCTS RTR-1500 experimental system was used to conduct proppant embedding tests for shale and sandstone, respectively (Pan et al., 2022). The implementation standard is Q/SY 17125-2019 "Performance Index and Evaluation Test Method of Fracturing Proppant." The cores used for the experiments were cylindrical samples with a diameter of 2.54 cm and a height of 2.5–3.0 cm, as shown in Figure 3, and two shale samples were stacked on the top and bottom with a certain amount of proppant placed in between. The proppant selected was the 10–20-mesh quartz sand proppant. The experimental results are shown in Figures 4, 5, where the effects of five closing stresses (10.0, 20.0, 30.0, 40.0, and 50.0 MPa) and five sand laying concentrations (6.0, 8.0, 10.0, 12.0, and 14.0 kg/m^2) are considered.

As can be seen from Figures 4, 5, with the increase in the closing pressure and the decrease in the laying concentration, the embedding depth of the proppant gradually increases. For shale, the embedding depth of the proppant is greater than that of sandstone under different conditions. With the increase in the closing pressure and the decrease in the sand concentration, the difference in the embedding depth between shale and sandstone becomes smaller. At the same time, it can be seen that the embedding depth of laminated shale is the largest, the foliation type is the second, and the sandwich type is the lowest; because the strength of laminated shale is the lowest, the proppant is more easily embedded.

5.2 Proppant conductivity

The DLY-III fracture conductivity tester was used to test the propped fracture conductivity, and the standard SY/T6302-2009 was implemented. The sample for the conductivity experiments is an elliptical slab formed from a full-diameter core in the study area with a long axis length of 15.80 cm and a sample thickness of 3.00 cm. The proppant used is a 10–20-mesh quartz sand proppant. The experimental results are shown in Figure 6, where the effects of five sand laying concentrations (6.0, 8.0, 10.0, 12.0, and 14.0 kg/m^2) are considered.

As shown in Figure 6, with the increase in the proppant laying concentration, the overall conductivity tends to increase, and the increase rate in conductivity gradually increases. In addition, it can also be seen that the sandwich shale has the strongest conductivity, followed by foliated shale, and the conductivity of laminated shale is the lowest; all of them are lower than the conductivity of sandstone.

6 Discussion

6.1 Influence of coring angles on shale mechanical properties

Figures 7–9 respectively, show the influence of the coring angle on elastic modulus, Poisson's ratio, and strength of the three types of shales.

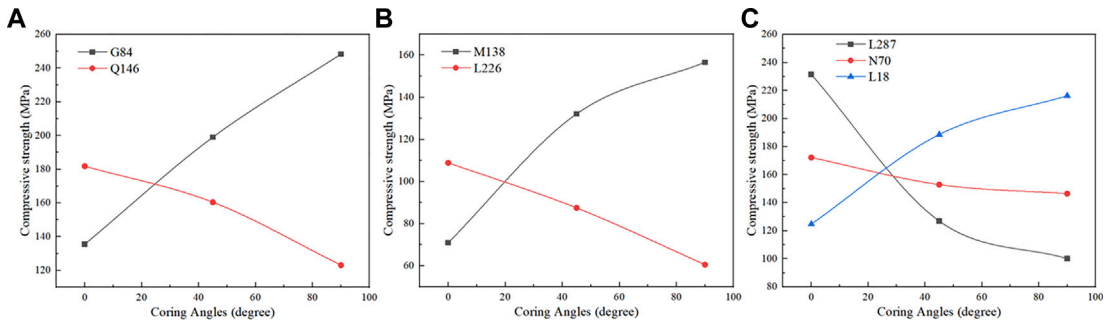

FIGURE 9
Influence of coring angle on compressive strength of different shale types. **(A)** Sandwich Shale, **(B)** Laminated Shale, **(C)** Foliated Shale.

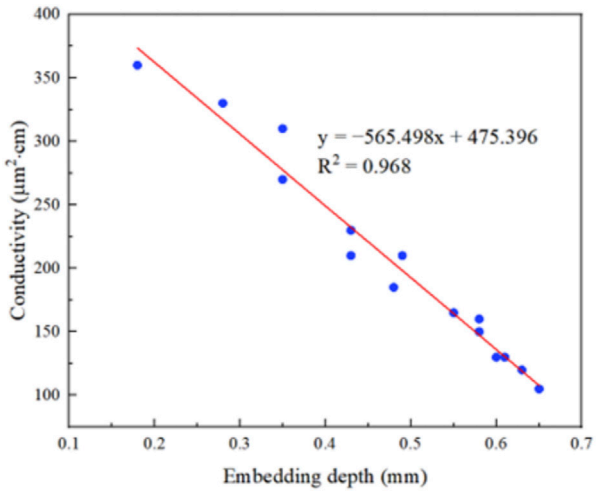

FIGURE 10
Correlation of the proppant embedding depth and proppant conductivity.

In the experiment, the coring angle refers to the angle between the direction of coring and the direction of the wellbore in a vertical well. The coring angle of 90 indicates that it is vertical to the wellbore direction and parallel to the bedding direction. By analyzing the influence of the coring angle, the characteristics of different types of shales are clarified and specific development methods are then adopted for different types of shales to make full use of different types of shale resources. It can be seen from Figure 7 that the elastic modulus of different types of shales increases with the increase in the coring angle and that the elastic modulus of cores in the direction of parallel bedding is the highest. Poisson's ratio of sandwich shale increases with the increase in the coring angle, as shown in Figure 8A, while for laminated and foliated shales, with the increase in the coring angle, there is no obvious regularity in the change of Poisson's ratio, as shown in Figure 8B,C. It can be seen from Figure 9 that the compressive strength of three kinds of shale has no obvious relation with the coring angle increase. The analysis is mainly due to the strong anisotropy and heterogeneity of shale, which shows that Poisson's ratio and compressive strength do not change with the coring angle. Based on the effect of mechanical inhomogeneity on the fracture shape (Xie et al., 2018), it is recommended that directional perforation along vertical bedding or a high angle should be preferred for foliated and laminated shales in Longdong, which is a favorable orientation for directional perforation, supplemented by partial spiral perforation, forming complex fractures and reducing invalid perforation.

6.2 Brittleness index

The brittleness index is a useful method for evaluating reservoir fracturability. There are many methods for calculating the brittleness index based on different fields, different problems, and different testing methods (Li, 2022; Zhang et al., 2022; Yang et al., 2023). Different calculation methods consider different factors and take different amounts of time and cost to evaluate brittleness. In order to save time and cost, a combination of laboratory experiments and logging data was adopted for brittleness evaluation. It is assumed that shale brittleness is only related to elastic properties such as elastic modulus and Poisson's ratio based on our previous research (Dou et al., 2022a). The calculation formula is as follows (Rickman et al., 2008):

$$Brit = 0.5\frac{(E - E_{min})}{E_{max} - E_{min}} + 0.5\frac{(\mu_{max} - \mu)}{\mu_{max} - \mu_{min}}, \quad (1)$$

where *Brit* represents the brittleness index; E represents the elastic modulus, MPa; E_{max} and E_{min} represent the maximum and minimum elastic moduli, MPa; μ represents the Young's modulus; μ_{max} and μ_{min} represent the maximum and minimum Young's moduli.

According to the logging data, the elastic modulus, and Poisson's ratio obtained from the experiment, the brittleness index for different types of shales in the study area is obtained and shown in Table 3. It can be seen from Table 3 that the laminated shale has the largest brittleness index (average is 0.56), followed by sandwich (average is 0.52), and foliated shales has the smallest brittleness index (average is 0.48). According to the brittleness index, it is inferred that the laminated and sandwich shales have stronger fracture-causing ability and are easy to form complex fracture networks.

According to the brittleness index corresponding to the mineral composition of different types of shales, it can be seen that the shales of lamellar and sandwich types have stronger brittleness and a higher rigid mineral content, which has a good corresponding relationship. When there is no brittleness experiment, the brittleness of a rock can be predicted by using the content of mineral components (Wei et al., 2022).

6.3 Fracture toughness

Fracture toughness is an important factor reflecting the difficulty level of reservoir modification and reflects the ability to maintain fracture extension forward after fracture formation during the fracturing process. Fracture damage during the network fracturing in shale reservoirs is dominated by type I (open) and type II (plane shear) (Dou et al., 2021a; Dou et al., 2022a). The fracture toughness is calculated as follows (Chen et al., 2015):

$$K_{IC} = 0.2176P_c + 0.0059S_t^3 + 0.0923S_t^2 + 0.517S_t - 0.3322, \quad (2)$$

$$K_{IIC} = 0.0956P_c + 0.1383S_t - 0.082, \quad (3)$$

$$P_c = \sigma_h - \alpha P_p. \quad (4)$$

Here, K_{IC} represents the fracture toughness of type I, MPa·m$^{0.5}$; K_{IIC} represents the fracture toughness of type II, MPa·m$^{0.5}$; S_t represents the tensile strength of the rock, MPa; P_c represents the surrounding pressure, MPa; α represents the effective stress factor, 0–1; P_p represents the porosity pressure, MPa; σ_h represents the minimum horizontal *in situ* stress, MPa.

Fracture toughness is also expressed using the normalized index:

$$K_n = 0.5\frac{K_{IC} - K_{ICmin}}{K_{ICmax} - K_{ICmin}} + 0.5\frac{K_{IIC} - K_{IICmin}}{K_{IICmax} - K_{IICmin}}, \quad (5)$$

where K_n represents the normalized index of fracture toughness, dimensionless; K_{ICmax} and K_{ICmin} represent the maximum and

minimum fracture toughness ranges of type I in the region, MPa·m$^{0.5}$; K_{IICmax} and K_{IICmin} represent the maximum and minimum fracture toughness ranges of type II in the region, MPa·m$^{0.5}$.

According to the logging data and the experiment data, fracture toughness for different types of shale in the study area is obtained and shown in Table 4. It can be seen from Table 4 that the sandwich shale has the smallest fracture toughness (average is 0.18) and that the fracture toughness of foliated and laminated shales is relatively larger (average is 0.42 and 0.415, respectively). The smaller the formation fracture toughness, the greater is the ability of the hydraulic fracture to penetrate the formation rock and the larger is the reservoir transformed volume. When fracture toughness of the formation is small, the natural fractures that are not in the extension path of hydraulic fractures are very likely to develop shear damage under the induced stress of hydraulic fractures, and a complex fracture network will be formed once the hydraulic fractures effectively communicate with the natural fractures. Therefore, according to the fracture toughness of different types of shales, sandwich shales are relatively easier to communicate than natural fractures, forming a complex fracture network and increasing the volume of transformation (Li et al., 2019; Guo et al., 2022).

6.4 Correlation of the proppant embedding depth and proppant conductivity

As shown in Figure 10, the proppant conductivity is inversely correlated with the proppant embedding depth; the deeper the proppant embedding depth, the weaker the proppant conductivity, and the correlation coefficient (R2) is 0.968. This is because the proppant embedding will reduce the width of the proppant fracture, and the deeper the proppant embedding, the more the width of the proppant fracture will be reduced.

7 Conclusion

There are three kinds of shales in the Ordos Basin, namely, laminated, sandwich, and foliated shales. In this paper, the three different types of shales are studied in terms of mineral composition, mechanical properties, and conductivity, compared with neighboring sandstones. The following conclusions were obtained, which provide some technical guidance for the identification of different types of shale fracturing desserts and fracturing processes.

(1) The foliated shale has the lowest content of rigid minerals (47.5%), lower elastic modulus and tensile strength (26.98 Gpa and 168.29 MPa, respectively), higher Poisson's ratio (0.25), the smallest brittleness index (0.48), and larger fracture toughness (0.42), reflecting that it is easier for the foliated shale to initiate fracture during fracturing, but fracture extension to form a complex fracture network is more difficult, and the fracturing effect is unsatisfactory.

(2) The laminated shale has a higher content of rigid minerals (68.50%), the lowest elastic modulus and tensile strength (25.77 Gpa and 122.46 MPa, respectively), the highest Poisson's ratio (0.26), the highest brittleness index (0.56), and the lowest fracture toughness (0.18), reflecting that it is easy for the laminated shale to initiate fracture during fracturing, and it is easier for fracture to expand to form a complex fracture network, and the fracturing effect is better.

(3) The sandwich shale has the highest rigid mineral content (78.16%), the highest elastic modulus and tensile strength (35.31 Gpa and 197.37 MPa, respectively), the lowest Poisson's ratio (0.24), larger brittleness index (0.52), and larger fracture toughness (0.415), reflecting that the sandwich shale requires a higher fracture initiation pressure during fracturing, but it is easier to form a complex fracture network, and the fracturing effect is better.

(4) With the increase in the coring angle, the elastic modulus of all three shales increases, and the Poisson's ratio of the sandwich shale increases, while the Poisson's ratio of the laminated and foliated shales and the compressive strength of the three shales have no relation with the coring angle increase. It is recommended to prefer directional injection along vertical laminae or at high angles, which is conducive to the formation of complex fracture networks.

(5) The proppant embedding depth gradually increases with the increase in the closing pressure and the decrease in the sand laying concentration. Meanwhile, the conductivity gradually increases with the increase in the laying concentration. The proppant embedding depth is deeper, and the conductivity is lower. For laminated shales with low strength, the sand laying concentration should be increased to ensure the conductivity of the fractured fracture.

Data availability statement

The original contributions presented in the study are included in the article/Supplementary Material; further inquiries can be directed to the corresponding author.

Author contributions

Conceptualization: LD and JC; methodology: LD; validation: JC, XZ, and YL; formal analysis: LS; investigation: YF; resources: LD; data curation: JC; writing—original draft preparation: JC; writing—review and editing: LD and XZ; visualization: YL; supervision: XC; project administration: TW; funding acquisition: LD. All authors contributed to the article and approved the submitted version.

Funding

This research was funded by the National Natural Science Foundation of China (no. 52074221), the Foundation of Key Laboratory of Unconventional Oil and Gas Development [China University of Petroleum (East China)] (no. 19CX05005A-203), the

Innovation Capability Support Program of Shaanxi (no. 2022KJXX-63), the Scientific Research Key Program Funded by Shaanxi Provincial Education Department (no. 21JY036), and the Postgraduate Innovation and Practice Ability Development Fund of Xi'an Shiyou University (no. YCS23113031).

Conflict of interest

Author LS was employed by the company Bohai Drilling Third Drilling Company of China Petroleum Group. Author YL was employed by the company Longdong Oil and Gas Development Branch of Changqing Oilfield.

The remaining authors declare that the research was conducted in the absence of any commercial or financial relationships that could be construed as a potential conflict of interest.

Publisher's note

All claims expressed in this article are solely those of the authors and do not necessarily represent those of their affiliated organizations, or those of the publisher, the editors, and the reviewers. Any product that may be evaluated in this article, or claim that may be made by its manufacturer, is not guaranteed or endorsed by the publisher.

References

Camargo, J. A. J., Cerca, M., and Carreon-Freyre, D. (2022). Microstructural effects on the unconfined mechanical behavior of a tectonically deformed calcareous shale, a study case in the Santiago Formation, México. *J. Petroleum Sci. Eng.* 217, 110856. doi:10.1016/J.PETROL.2022.110856

Chen, J., Deng, J., Yuan, J., Sumanovski, L. T., Schneider, B. L., and Helmchen, F. (2015). Pathway-specific reorganization of projection neurons in somatosensory cortex during learning. *Chin. J. Rock Mech. Eng.* 34 (6), 1101–1108. doi:10.1038/nn.4046

Cho, J. W., Kim, H., Jeon, S., and Min, K. B. (2012). Deformation and strength anisotropy of Asan gneiss, Boryeong shale, and Yeoncheon schist. *Int. J. rock Mech. Min. Sci.* 50, 158–169. doi:10.1016/j.ijrmms.2011.12.004

da Silva, M. R., Schroeder, C., and Verbrugge, J. C. (2008). Unsaturated rock mechanics applied to a low-porosity shale. *Eng. Geol.* 97 (1-2), 42–52. doi:10.1016/j.enggeo.2007.12.003

Dou, L., Chen, J., Li, N., Bai, J., Fang, Y., Wang, R., et al. (2022b). Quantitative evaluation of imbibition damage characteristics of foaming agent solutions in shale reservoir. *Energies* 15 (16), 5768. doi:10.3390/EN15165768

Dou, L., Shu, G., Gao, H., Bao, J., and Wang, R. (2021b). Study on the effect of high-temperature heat treatment on the microscopic pore structure and mechanical properties of tight sandstone. *Geofluids* 2021, 1–13. doi:10.1155/2021/8886186

Dou, L., Xiao, Y., Gao, H., Wang, R., Liu, C., and Sun, H. (2021c). The study of enhanced displacement efficiency in tight sandstone from the combination of spontaneous and dynamic imbibition. *J. Petroleum Sci. Eng.* 199, 108327. doi:10.1016/J.PETROL.2020.108327

Dou, L., Yang, H., Xiao, Y., et al. (2021a). A new method for evaluating the brittleness and fracturability of shale reservoirs. *Prog. Geophys.* 36 (2), 576–584. doi:10.6038/pe2021EE0460

Dou, L., Zuo, X., Qu, L., Xiao, Y., Bi, G., Wang, R., et al. (2022a). A new method of quantitatively evaluating fracability of tight sandstone reservoirs using geomechanics characteristics and *in situ* stress field. *Processes* 10 (5), 1040. doi:10.3390/PR10051040

Du, X. (2023). Fractal characteristics of sandwich shale oil reservoir in Chang 7 member of Longdong area and its relationship with pore structure and oil-bearing property. *J. Yangtze Univ. Nat. Sci. Ed.* 20 (1), 38–47. doi:10.16772/j.cnki.1673-1409.2023.01.002

Fu, Q., Liu, Q., and Liu, S., (2019). Exploration and development status and prospect of sandwich-type shale oil reservoirs in China. *Oil Drill. Prod. Technol.* 41 (1), 63–70. doi:10.13639/j.odpt.2019.01.011

Gallant, C., Zhang, J., Wolfe, C. A., Freeman, J., Al-Bazali, T., and Reese, M. "Wellbore stability considerations for drilling high-angle wells through finely laminated shale a case study from Terra Nova," in Proceedings of the SPE Annual Technical Conference and Exhibition, Anaheim, California, USA, 2007, November. doi:10.2118/110742-MS

Guo, Y., Wang, D., Han, X., Zhang, K., Shang, X., and Zhou, S. (2022). Evaluation of fracturability of shale reservoirs in the longmaxi formation in southern sichuan basin. *Front. Earth Sci.* 10, 993829. doi:10.3389/FEART.2022.993829

Horsrud, P. (2001). Estimating mechanical properties of shale from empirical correlations. *SPE Drill. Complet.* 16 (02), 68–73. doi:10.2118/56017-PA

Jia, J., Zhong, A., Zhang, Z., et al. (2021). Numerical simulation study on brittleness anisotropy of marly shale in Jiyang Depression. *Pet. Drill. Technol.* 49 (4), 78–84. doi:10.11911/syztjs.2021086

Lee, J. S., Smallwood, L., and Morgan, E. "New application of rebound hardness numbers to generate logging of unconfined compressive strength in laminated shale formations," in Proceedings of the 48th US Rock Mechanics/Geomechanics Symposium, Minneapolis, Minnesota, United States, June 2014. doi:10.2807/1560-7917.ES2014.19.30.20864

Li, H. (2022). Research progress on evaluation methods and factors influencing shale brittleness: a review. *Energy Rep.* 8, 4344–4358. doi:10.1016/J.EGYR.2022.03.120

Li, H., Tang, H., Qin, Q., Zhou, J., Qin, Z., Fan, C., et al. (2019). Characteristics, formation periods and genetic mechanisms of tectonic fractures in the tight gas sandstones reservoir: a case study of xujiahe formation in yb area, sichuan basin, china. *J. Petroleum Sci. Eng.* 178, 723–735. doi:10.1016/j.petrol.2019.04.007

Liang, M., Wang, Z., Zheng, G., Zhang, X., Greenwell, H. C., Zhang, K., et al. (2021). Preliminary experimental study of methane adsorption capacity in shale after brittle deformation under uniaxial compression. *Front. Earth Sci.* 9, 542912. doi:10.3389/FEART.2021.542912

Liu, B., Sun, J., Zhang, Y., He, J., Fu, X., Yang, L., et al. (2021). Reservoir space and enrichment model of shale oil in the first member of Cretaceous Qingshankou Formation in the Changling sag, southern Songliao Basin, NE China. *Petroleum Explor. Dev.* 48 (3), 608–624. doi:10.1016/s1876-3804(21)60049-6

Liu, S. (2019). Analysis of the influence of foliation on logging response and rock mechanics parameters. *Unconv. Oil Gas* 6 (4), 1–5.

Liu, Y., and Liu, P. (2019). Interlayer characteristics and their effect on continental facies organic-rich shale: a case study of jiyang depression. *Editor. Dep. Petroleum Geol. Recovery Effic.* 26 (5), 1–9. doi:10.13673/j.cnki.cn37-1359/te.2019.05.001

Pan, L., Wang, H., and He, J., (2022). Experimental study on the influence of shale hydration on proppant embedding. *Sci. Technol. Eng.* 22 (13), 5228–5235.

Pang, Z., Tao, S., and Zhang, Q., (2023). Oil enrichment law and main controlling factors of sandwich shale series in member 7 of Yanchang Formation in Ordos Basin. *Earth Sci. Front.* 30 (4), 152–163. doi:10.13745/j.esf.sf.2022.10.17

Rickman, R., Mullen, M., Petre, E., Grieser, B., and Kundert, D. "A practical use of shale petrophysics for stimulation design optimization: all shale plays are not clones of the barnett shale," in Prceedings of the SPE Annual Technical Conference and Exhibition, Denver, Colorado, USA, September 2008. doi:10.2118/115258-MS

Ruggieri, R., Scuderi, M. M., Trippetta, F., Tinti, E., Brignoli, M., Mantica, S., et al. (2021). The role of shale content and pore-water saturation on frictional properties of simulated carbonate faults. *Tectonophysics* 807, 228811. doi:10.1016/J.TECTO.2021.228811

Shen, R., Xiong, W., Yang, H., Zeng, X., Wang, G., and Shao, G. (2022). Study on fluid mobility in sandwich-type shale oil reservoir using two-dimensional nuclear magnetic resonance approaches. *Energy Sources, Part A: recovery, util. environ. eff.* 44 (3), 5951–5967. doi:10.1080/15567036.2022.2094503

Simpson, N. D. J., Stroisz, A. N. N. A., and Bauer, A., "Failure mechanics of anisotropic shale during Brazilian tests," in Proceedings of the ARMA US Rock Mechanics/Geomechanics Symposium, Minneapolis, Minnesota, United States, June 2014.

Song, S., Chen, S., and Yan, J., (2023). Structural types of shale laminae in the second member of Kongdong sag and their influence on reservoir performance. *J. gansu Sci.* 35 (1), 1–9. doi:10.16468/j.cnki.issn1004-0366.2023.01.001

Sun, L., Liu, H., He, W., Li, G., Zhang, S., Zhu, R., et al. (2021). An analysis of major scientific problems and research paths of Gulong shale oil in Daqing Oilfield, NE China. *Petroleum Explor. Dev.* 48 (3), 527–540. doi:10.1016/S1876-3804(21)60043-5

Tan, P., Jin, Y., Han, K., Hou, B., Chen, M., Guo, X., et al. (2017). Analysis of hydraulic fracture initiation and vertical propagation behavior in laminated shale formation. *Fuel* 206, 482–493. doi:10.1016/j.fuel.2017.05.033

Tang, X., Xu, H., and Cao, Y., (2022). Geological characteristics of limestone sandwich shale oil in the second member of Sanshui Basin. *Petroleum Geol. Eng.* 36 (2), 48–53.

Teng, J., Qiu, L., Zhang, S., and Ma, C. (2022). Origin and diagenetic evolution of dolomites in paleogene Shahejie Formation lacustrine organic shale of jiyang depression, bohai bay basin, east China. *Petroleum Explor. Dev.* 49 (6), 1251–1265. doi:10.1016/s1876-3804(23)60347-7

Tian, T., Fu, D., and Yang, F., (2018). Relationship between shale mineral composition and micropores in Niutitang Formation in micangshan-hannan uplift area. *J. Coal Sci.* 43 (S1), 236–244. doi:10.13225/j.cnki.jccs.2017.1646

Valdiviezo-Mijangos, O. C., and Nicolás-Lopez, R. (2014). Dynamic characterization of shale systems by dispersion and attenuation of P-and S-waves considering their mineral composition and rock maturity. *J. Petroleum Sci. Eng.* 122, 420–427. doi:10.1016/j.petrol.2014.07.041

Wakabayashi, J., and Dilek, Y. (2011). Mélanges of the Franciscan Complex, California: diverse structural settings, evidence for sedimentary mixing, and their connection to subduction processes. *Mélanges: process. form. soc. significance* 480, 117–141. doi:10.1130/2011.2480(05

Wang, J., Gong, J., and Zhang, L. (2018c). Discussion on preservation conditions of shale gas with "Sandwich" structure in South Yellow Sea basin. *Mar. Geol. Quat. Geol.* 38 (3), 134–142. doi:10.16562/j.cnki.0256-1492.2018.03.013

Wang, J., Gong, J., Zhang, L., Cheng, H. y., Liao, J., Chen, J. w., et al. (2018a). Discussion on "sandwich" structures and preservation conditions of shale gas in the South Yellow Sea Basin. *China Geol.* 1 (4), 485–492. doi:10.31035/cg2018064

Wang, K., Li, K., and Wang, L., (2018b). Mineral composition and gas-bearing characteristics of shale of Wufeng-Longmaxi Formation in Shizhu area, eastern margin of Sichuan Basin. *J. Lanzhou Univ. Nat. Sci. Ed.* 54 (03), 285–291+302. doi:10.13885/j.issn.0455-2059.2018.03.001

Wei, Y., Zhao, L., Yuan, T., and Liu, W. (2022). Study on mechanical properties of shale under different loading rates. *Front. Earth Sci.* 9, 815616. doi:10.3389/FEART.2021.815616

Xie, J., Jiang, G., and Wang, R., (2018). Experimental investigation on the influence of perforation on the hydraulic fracture geometry in shale. *J. China Coal Soc.* 43 (3), 776–783. doi:10.13225/j.cnki.jccs.2017.0944

Xin, B., Zhao, X., Hao, F., Jin, F., Pu, X., Han, W., et al. (2022). Laminae characteristics of lacustrine shales from the Paleogene Kongdian Formation in the Cangdong Sag, Bohai Bay Basin, China Why do laminated shales have better reservoir physical properties? *Int. J. Coal Geol.* 260, 104056. doi:10.1016/J.COAL.2022.104056

Xiong, M., Chen, L., and Chen, X., (2022). Characteristics, genetic mechanism and shale gas significance of marine shale. *J. Central South Univ. Nat. Sci. Ed.* 53 (9), 3490–3508. doi:10.11817/j.issn.1672-7207.2022.09.016

Xu, J., Guoxin, L., Siwei, M., Wang, X., Liu, C., Tao, J., et al. (2021). Microscale comprehensive evaluation of continental shale oil recoverability. *Petroleum Explor. Dev.* 48 (1), 256–268. doi:10.1016/S1876-3804(21)60021-6

Yang, C., Wu, Z., Wang, W., Qu, H., Ren, N., and Li, H. (2023). Study on the influence of natural cracks on the mechanical properties and fracture mode for shale at the microscale: an example from the lower cambrian niutitang formation in northern guizhou. *Front. Earth Sci.* 10, 1032817. doi:10.3389/FEART.2022.1032817

Yang, H., Niu, X. B., Xu, L. M., Feng, S., You, Y., Liang, X., et al. (2016). Exploration potential of shale oil in Chang7 member, upper Triassic Yanchang formation, Ordos Basin, NW China. *Petroleum Explor. Dev.* 43 (4), 560–569. doi:10.1016/S1876-3804(16)30066-0

Yang, J., Gong, B., and Zhou, Y., (2021). HSP70 and FLT3-ITD: targeting chaperone system to overcome drug resistance. *Daqing Petroleum Geol. Dev.* 40 (03), 151–153. doi:10.1097/BS9.0000000000000094

Zhang, D., Tang, J., Chen, K., Wang, K., Zhang, P., He, G., et al. (2022). Simulation of tectonic stress field and prediction of tectonic fracture distribution in Longmaxi Formation in Lintanchang area of eastern Sichuan Basin. *Front. Earth Sci.* 10, 1024748. doi:10.3389/FEART.2022.1024748

Zhang, J., Al-Bazali, T., and Chenevert, M., "Compressive strength and acoustic properties changes in shale with exposure to water-based fluids," in Proceedings of the ARMA US Rock Mechanics/Geomechanics Symposium, Golden, Colorado, USA, June 2006.

Zhang, J., Xie, Z., Pan, Y., Tang, J., and Li, Y. (2023). Synchronous vertical propagation mechanism of multiple hydraulic fractures in shale oil formations interlayered with thin sandstone. *J. Petroleum Sci. Eng.* 220, 111229. doi:10.1016/J.PETROL.2022.111229

Zhao, X., Yan, J., and Hu, Q., (2021). Study on the rock mechanical characteristics of different laminae of marine shale and its significance-taking the Wufeng Formation-Longmaxi Formation in LZ area of Sichuan Basin as an example. *Abstr. 16th Natl. Symposium Paleogeogr. Sedimentology* 179. doi:10.26914/c.cnkihy.2021.016716

Zhao, X., Yan, J., and Wang, M., (2022). Sandwich characteristics and logging identification method of lacustrine shale in Shahejie Formation of Zhanhua Depression. *Lithologic Oil Gas Reserv.* 34 (1), 118–129. doi:10.12108/yxyqc.20220112

Zhu, C., Sheng, J. J., Ettehadtavakkol, A., Li, Y., and Dong, M. (2019). Numerical and experimental study of oil transfer in laminated shale. *Int. J. Coal Geol.* 217, 103365. doi:10.1016/j.coal.2019.103365

Zhu, D., Wang, Y., and Zhu, D., (2015). Definition criteria and main controlling factors of shale oil enrichment in Shahejie Formation in Bonan Depression. *Oil gas Geol. recovery* 22 (5), 15–20. doi:10.13673/j.cnki.cn37-1359/te.2015.05.001